

Electroreflectance, Absorption Coefficient, and Energy-Band Structure of CdGeP₂ near the Direct Energy Gap

J. L. Shay

Bell Telephone Laboratories, Holmdel, New Jersey 07733

and

E. Buehler and J. H. Wernick

Bell Telephone Laboratories, Murray Hill, New Jersey 07974

(Received 24 May 1971)

We report electroreflectance and absorption measurements near the direct energy gap of CdGeP₂ at 1.72 eV. The ordering, splittings, and polarization properties of the three closely spaced energy gaps derived from $\Gamma_{15} \rightarrow \Gamma_1$ in zinc-blende crystals are quantitatively explained by a quasicubic model taking into account the built-in uniaxial compression alone. Although the absorption coefficient is ~ 45 times larger for $\vec{E} \parallel Z$, at low temperatures we observe in the absorption spectrum for $\vec{E} \perp Z$, a free exciton with a binding energy of 7.7 meV near the lowest energy gap. The observation of this exciton is independent evidence that the dichroism of the absorption edge in II-IV-V₂ crystals results entirely from the lowest energy gap having a highly anisotropic oscillator strength. The dichroism of the absorption edge is opposite to that recently assumed by Goryunova *et al.* in the process of optically orienting single crystals. Hence their conclusion that CdGeP₂ is negatively birefringent is in error, and in fact, CdGeP₂ is positively birefringent (extraordinary index larger than ordinary index). After allowing for this sign error, we show that the dispersion of the birefringence of CdGeP₂ can be readily explained by a theoretical model, taking into account the built-in uniaxial compression alone.

I. INTRODUCTION AND CONCLUSIONS

As the closest ternary analogs of III-V zinc-blende crystals, the II-IV-V₂ chalcopyrite semiconductors are currently being investigated for their possible application as junction lasers in the visible region of the spectrum and as candidates for optical parametric oscillators. An attractive feature of the chalcopyrite crystal system is that one can predict properties of these ternary crystals by extrapolating from the well-understood binary zinc-blende crystals. Many of their properties can be understood by a simple analogy. For example, the direct band gaps of CdSnP₂^{1,2} (1.17 eV), ZnSiAs₂³ (2.12 eV), CdSiAs₂⁴ (1.55 eV), and CdGeP₂ (1.72 eV) lie within 0.3 eV of the band gaps of their III-V analogs. The lowest direct gap in a chalcopyrite crystal is one of three closely spaced energy gaps derived from the triply degenerate $\Gamma_{15} \rightarrow \Gamma_1$ transition in its cubic binary analog. The degeneracy is completely lifted in chalcopyrite crystals by the simultaneous effects of spin-orbit interaction and the uniaxial crystal potential. It has recently been shown¹⁻⁵ that the ordering and spacings of these valence bands (e.g., in CdSnP₂) are identical to those which would obtain in the stressed binary analog (e.g., InP) could one stress the binary crystal sufficiently to achieve the uniaxial lattice distortion present in the ternary crystal. The quantitative success of this simple quasicubic model is surprising since it ignores two other

noncubic aspects of chalcopyrite crystals which could have been equally as important. In addition to the built-in uniaxial compression, the other noncubic aspects of the chalcopyrite structure are (a) an internal strain arising from the systematic distortion of the anions away from the $\frac{1}{4} \frac{1}{4} \frac{1}{4}$ sites in such a way as to reduce the IV-V bond lengths and (b) the presence of two different cations alternately located on the cation sites of the analogous zinc-blende structure.

We have initiated the present study of CdGeP₂ because, as the ternary analog of $\frac{1}{2}$ (InP + GaP), it should have the largest direct energy gap of any II-IV-V₂ chalcopyrite crystal. All other II-IV-V₂ compounds with larger direct gaps (such as ZnGeP₂, an analog of GaP) are expected to have lower-lying indirect and pseudodirect energy gaps. The latter are direct energy gaps which correspond to indirect energy gaps in zinc-blende crystals but become direct in chalcopyrite crystals by virtue of the imbedding of the zinc-blende Brillouin zone into the smaller, chalcopyrite Brillouin zone.⁶ As anticipated by the binary-ternary analogy, we find from electroreflectance measurements that CdGeP₂ has a direct energy gap at 1.72 eV, and that the ordering and splitting of the three valence bands corresponding to Γ_{15} in cubic crystals are quantitatively explained by the quasicubic model. We observe a sharp absorption edge at the direct energy gap which suggests that there are no lower-lying indirect energy gaps.

In a recent study of CdSnP_2 ,⁷ the dichroism of the absorption edge and the dispersion of the birefringence were shown to be the result of the built-in uniaxial distortion. In the present work, we find that the same conclusions apply to CdGeP_2 . The dichroism of the absorption edge is opposite to that assumed by Goryunova *et al.*⁸ in the process of optically orienting single crystals for the purpose of measuring refractive indices. Hence their result that CdGeP_2 is negatively birefringent is in error, and, in fact, CdGeP_2 is positively birefringent ($n_e > n_o$). After allowing for this sign error, we show that the dispersion of the birefringence measured by Goryunova *et al.*⁸ is explained by a theoretical model accounting for the built-in uniaxial compression alone. The asymptotic value of the birefringence at long wavelengths is not dominated by the built-in uniaxial compression, since compression of a large-bandgap zinc-blende crystal such as GaP produces a negative birefringence at long wavelengths, whereas the birefringence of CdGeP_2 is positive. Clearly, one of the other noncubic aspects of the chalcopyrite structure is dominating the long-wavelength birefringence. Though positive, the birefringence is large (≥ 0.12) and may permit phase-matched optical parametric oscillation.

The previously mentioned study⁷ of CdSnP_2 revealed that the dichroism of the absorption edge results entirely from a single electronic transition (the lowest-energy gap) having a highly anisotropic oscillator strength. Hence, the shape of the absorption edge (energy dependence) is independent of the polarization of the incident radiation. We have independently verified this conclusion by observing an exciton in the absorption spectrum of CdGeP_2 near the lowest-energy gap, for the weak-absorption polarization $\vec{E} \perp z$.

Other than the refractive-index measurements⁸ mentioned earlier, the only previous study of the optical properties of crystalline CdGeP_2 is a measurement of the spectral dependence of the photoconductivity⁹ from which it was estimated that the energy gap was about 1.8 eV, in agreement with our electroreflectance measurements (1.72 eV). Single crystals of CdGeP_2 are somewhat difficult to prepare because of a glassy phase¹⁰⁻¹² having an energy gap near 0.8 eV. Nonetheless we have shown that crystalline CdGeP_2 has a direct energy gap larger than that of any III-V compound (except GaN and perhaps AlN) and therefore may be of interest as a junction emitter.

II. EXPERIMENTAL TECHNIQUES

Several preliminary attempts to grow sizable crystals of CdGeP_2 from the melt were unsuccessful because of the presence of cracks. Single crystals of CdGeP_2 were successfully grown from

the vapor phase using I_2 to transport the Ge. The resulting crystals were platelets with dimensions as large as $2 \times 5 \times 0.5 \text{ mm}^3$. X-ray power studies verified that the crystals had the chalcopyrite structure, and studies using a Laue camera and an x-ray goniometer identified the major facets as (011). Inspection under a polarizing infrared microscope revealed sharp uniform extinctions when the polaroids made at an angle of $\sim 24^\circ$ to the crystal edges as expected for (011) facets. Using a calcite compensator, it was verified that the birefringence of CdGeP_2 is positive. For an (011) orientation, incident radiation can be polarized with the electric vector perpendicular to the optic axis, but not completely parallel to this axis. Consequently, in the electroreflectance spectra $\vec{E} \parallel Z$ is only nominal, and, in fact, at most $\frac{4}{5}$ of the intensity lies parallel to Z .

The vapor-grown crystals were semi-insulating with resistances greater than $10^8 \Omega$ as measured with Ga-In contacts. Such a high resistance precluded electrolyte electroreflectance measurements, since the applied voltage would appear across the bulk of the crystal rather than the crystal-electrolyte interface. We therefore resorted to the transverse-electroreflectance technique¹³ in which an electric field is applied along the sample's surface. In the present work, gold electrodes were evaporated $\frac{1}{2}$ mm apart, perpendicular to the long edge of the (011) platelets which were typically $\frac{1}{4}$ mm thick and $\frac{1}{2}$ mm wide. Sinusoidal voltages up to 5 kV peak to peak at 510 Hz were applied between the gold electrodes, and the modulated reflectance was monitored at twice the modulating frequency (1020 Hz) with a lock-in amplifier. Incident radiation was polarized with an HN32 Polaroid. In the vicinity of the direct energy gap (7200 Å), a tungsten halogen lamp and a silicon photovoltaic detector were used (EGG model No. SGD444). The noise level in $\Delta R/R$ for these measurements was $\sim 2 \times 10^{-7}$. Beyond the cutoff of the silicon detector at 4000 Å, an S-20 photomultiplier was used together with a xenon lamp; however any signal was below the noise level of $\sim 10^{-5}$.

At room temperature, the absolute transmission was measured by the sample-in-sample-out technique using identical apertures. High spectral purity was assured by the use of a Jarrell-Ash double monochromator. Transmission measurements over the range 2–300 °K made use of a Janis variable-temperature stainless-steel Dewar.

III. EXPERIMENTAL RESULTS

A. Electroreflectance Measurements

The transverse-electroreflectance spectra of CdGeP_2 near the lowest direct energy gap is shown in Fig. 1 for light polarized, respectively, parallel

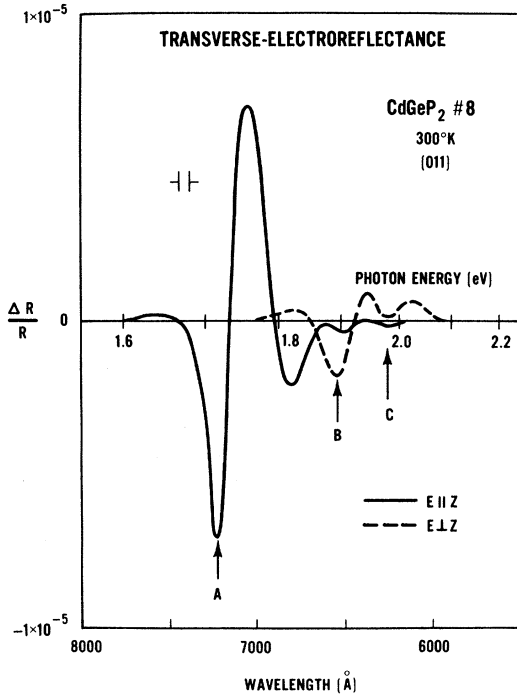


FIG. 1. Transverse-electroreflectance spectra near the direct energy gap of CdGeP₂ for light polarized, respectively, parallel and perpendicular to the optic axis. For an (011) platelet, $\vec{E} \parallel Z$ is only nominal, as explained in the text. $V_{ac} = 5.2$ kV_{pp} which corresponds to a peak field of about 50 kV/cm.

and perpendicular to the optic axis. The *A*, *B*, and *C* peaks at 1.72, 1.90, and 1.99 eV are attributed to transitions to a single conduction band from three closely spaced valence bands. As previously reported¹⁻⁵ for CdSnP₂, ZnSiAs₂, and CdSiAs₂, these three transitions in chalcopyrite crystals are derived from the $\Gamma_{15} \rightarrow \Gamma_1$ transition in zinc-blende crystals according to the model shown in Fig. 2. The triple degeneracy of the *p*-like Γ_{15} valence band is completely lifted in chalcopyrite under the simultaneous perturbations of spin-orbit coupling and the noncubic crystal potential. The group-theoretical selection rules are indicated in Fig. 2. Whereas the *B* peak is only allowed for $E \perp Z$, it is partially observed in the solid curve in Fig. 1 because of the experimental constraint that $E \parallel Z$ is only nominal, as explained earlier.

The ordering and splittings of the *A*, *B*, and *C* peaks can be explained by a simple model which approximates the valence bands of a chalcopyrite crystal as identical to those in a strained version of its hypothetical binary analog. Within this so-called quasicubic model,⁵ the energies of the Γ_7 valence-band levels relative to the Γ_6 level are given by^{14,15}

$$E_{1,2} = \frac{1}{2}(\Delta_{so} + \Delta_{cf}) \pm \frac{1}{2}[(\Delta_{so} + \Delta_{cf})^2 - \frac{8}{3}\Delta_{so}\Delta_{cf}]^{1/2}, \quad (1)$$

where Δ_{so} is the spin-orbit splitting of the Γ_{15} valence band in the binary analog and Δ_{cf} is the crystal field splitting parameter. Considering only the effects of the built-in compression of the chalcopyrite lattice, we estimate Δ_{cf} by

$$\Delta_{cf} = \frac{3}{2}b(2 - C/A), \quad (2)$$

where *b* is the deformation potential describing the splitting of the valence bands in the zinc-blende analog under uniaxial stress, and *C* and *A* are the chalcopyrite lattice constants.¹⁶ Equations (1) and (2) describe the splitting of the Γ_{15} valence band in zinc-blende crystals under the simultaneous effects of spin-orbit interaction and an externally applied uniaxial strain.¹⁷ The experimental parameters Δ_{so} and Δ_{cf} , determined from the splitting of the *A*, *B*, and *C* peaks using Eq. (1), are summarized in Table I together with the theoretical values predicted by the quasicubic model.¹⁸ We also include previously reported data for CdSnP₂, CdSiAs₂, and ZnSiAs₂, as well as the crystal field splitting predicted by a recent pseudopotential calculation.¹⁹ It can be seen in Table I that the agreement between the quasicubic model and experiment is quite good and that the pseudopotential calculation of Δ_{cf} is not noticeably closer to experiment than the simple results of Eq. (2). We therefore conclude that Eqs. (1) and (2) contain the essential physics of the valence-band splittings in II-IV-V₂ chalcopyrite crystals.

In addition to the eigenvalues given by Eq. (1), the quasicubic model determines eigenfunctions from which one can predict polarization dependences. For this model the ratio of the strengths of transitions from a given Γ_7 valence band to the Γ_6 conduction band for light polarized, respectively, parallel or perpendicular to the optic axis is given by^{14,15}

TABLE I. Comparison of theoretical and experimental values for the crystal field Δ_{cf} and spin-orbit Δ_{so} parameters which determine the ordering and splittings of the valence bands (in eV).

	CdSnP ₂ ^a	CdGeP ₂	CdSiAs ₂ ^b	ZnSiAs ₂ ^c
Δ_{so} Experiment	0.10	0.11	0.29	0.28
Δ_{so} Theory (quasicubic)	0.11	0.10	0.34	0.31
Δ_{cf} Experiment	-0.10	-0.20	-0.24	-0.13
Δ_{cf} Theory (quasicubic) ^d	-0.12	-0.27	-0.39	-0.15
Δ_{cf} Theory (pseudopotential) ^e	-0.14	-0.14	-0.29	-0.20

^aReference 2.

^bReference 4.

^cReference 3.

^dValues for ZnSiAs₂ and CdSiAs₂ are based on revised estimates of the deformation potential for GaAs taken from Ref. 18.

^eReference 19.

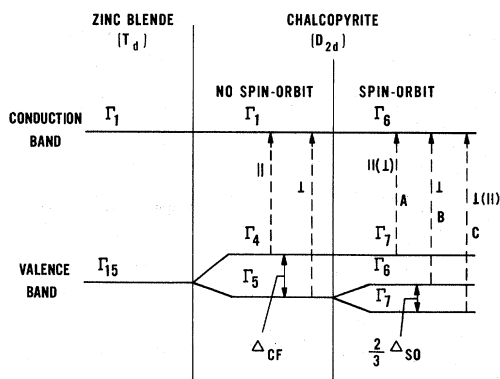


FIG. 2. Band-structure and selection rules for the three energy gaps in chalcopyrite crystals derived from the $\Gamma_{15} \rightarrow \Gamma_1$ energy gap in zinc-blende crystals (Ref. 1). The splittings and polarization dependences are indicated schematically for a crystal in which $\Delta_{so} \ll \Delta_{cf}$. For arbitrary values of these parameters, the splittings and polarization dependences are given, respectively, by Eqs. (1) and (3) in the text.

$$I_{\parallel}/I_{\perp} = (2 - 3E\Delta_{so})^2 \quad (3)$$

Using $E = -0.18$ and $\Delta_{so} = 0.11$, Eq. (3) predicts that $I_{\parallel}/I_{\perp} = 45$ for the A peak in CdGeP_2 , and this peak is therefore below the noise level in Fig. 1 for $E \perp Z$.

B. Absorption Measurements

In Fig. 3, we present the absorption coefficient of CdGeP_2 measured near the direct energy gap on a (011) platelet $75 \mu\text{m}$ thick. As expected from the valence-band model in Fig. 2 and the electroreflectance data in Fig. 1, the absorption coefficient near the A energy gap at 1.72 eV is considerably larger for the extraordinary ray ($E \parallel Z$) than for the ordinary ray ($E \perp Z$), where Z is the optic axis. Whereas the polarization ratio for the A transition is expected to be ~ 45 (Sec. III A), α_{\parallel} is only about five times larger than α_{\perp} at energies below the A energy gap at 1.72 eV . Since the spectrum of α_{\perp} is noticeably different from that of α_{\parallel} between $1.6\text{--}1.7 \text{ eV}$, we attribute the smaller polarization ratio to a polarization-independent contribution to the absorption coefficient (due to impurities) which masks the contribution from the A energy gap for $E \perp Z$.

In an earlier study of CdSnP_2 ,⁷ it was shown that the absorption coefficient near the A energy gap was dominated by transitions at the A energy gap for both polarizations of the radiation relative to the optic axis. It is therefore reasonable to attribute the rapid increase in α_{\perp} for photon energies greater than 1.7 eV to the onset of direct transitions associated with the A energy gap. The theoretical line shape for such a transition, ignoring for the moment

the Coulomb attraction of the electron and hole, is of the form²⁰

$$\alpha = \alpha_0 (h\nu - E_g)^{1/2}, \quad (4)$$

where E_g is the energy gap. The theoretical curve in Fig. 3 provides a good fit to the data for $E_g = 1.711 \text{ eV}$ and $\alpha_0 = 2400 \text{ cm}^{-1}/\text{eV}^{1/2}$.

There is reason for questioning the physical significance of the good agreement between theory and experiment indicated in Fig. 3. The energy gap determined from the fit to Eq. (4) is *less than* the energy of the A peak at 1.72 eV in the electroreflectance data (Fig. 1), whereas electroreflectance theory²¹ requires that the energy gap should lie at, or slightly *above*, the first negative peak depending upon the amount of spectral broadening. Furthermore, it is well known from studies of binary zinc-blende crystals (e.g., GaAs ²²) that the Coulomb attraction of electrons and holes modifies the shape of the absorption edge even at room temperature. Consequently, the true energy gap probably lies slightly above the value for E_g determined by the best fit of Eq. (4) to experiment. This conclusion is borne out in GaAs , in which modulated reflectance data²³ locate the room-temperature energy gap at 1.420 eV , but the fit of Eq. (4) to experiment results in $E_g = 1.41 \text{ eV}$.²⁴

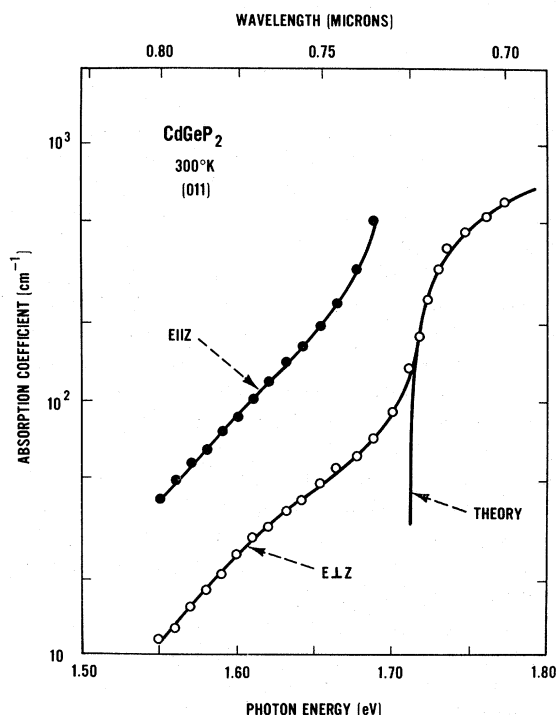


FIG. 3. Absorption coefficients for the extraordinary (solid circles) and ordinary rays (open circles) on a (011) platelet $75 \mu\text{m}$ thick. The theoretical curve is a fit of Eq. (4) to the data ignoring exciton effects.

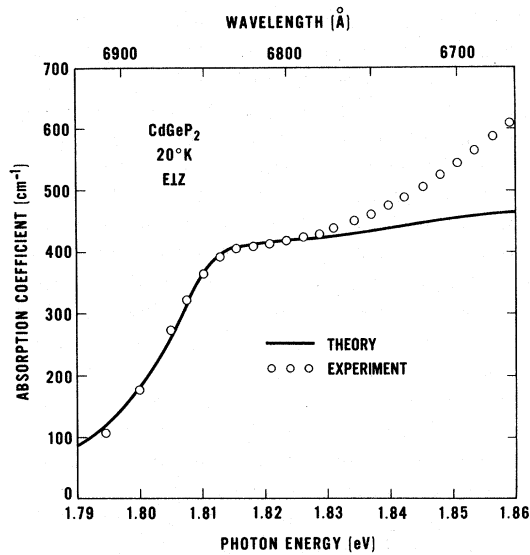


FIG. 4. Absorption coefficient measured for the ordinary ray at 20 °K (circles). The solid curve is a Lorentzian-broadened theoretical fit including discrete and continuum excitons (after Ref. 25). The parameters of the fit are $E_g=1.819$ eV, $R=7.7$ meV, $\Gamma=10.8$ meV. The deviation of the data from the theory above 1.83 eV results from the nonparabolicity of the valence bands and the onset of a broadened exciton at the next-higher gap ~ 0.18 eV above the lowest direct energy gap.

The contribution of excitons to the absorption edge of CdGeP₂ is more clearly seen at low temperatures, as shown in Fig. 4. The lowest bound state lies between 1.81 and 1.82 eV at the knee in the data, but is considerably broadened by residual impurities. In the absence of any broadening, the absorption edge would consist of a hydrogenic series of discrete lines at energies R/n^2 below the energy gap of the form $[1 - \exp(-2\pi z)]^{-1}$, where $z^2 = R/(E - E_g)$. R is the exciton rydberg and E_g is the energy gap. Sell and Lawaetz²⁵ have recently shown that the most reliable method for determining R from broadened experimental data, such as we have in Fig. 4, is to fit the data near the exciton peak (or knee) to a composite theoretical curve, including discrete and continuum excitons, broadened by a Lorentzian function $\Gamma\pi^{-1}(E^2 + \Gamma^2)^{-1}$, where 2Γ is the full width at half-maximum. The solid curve in Fig. 4 is an attempt to fit the data below 1.83 eV with such a broadened composite theoretical model. At 20 °K, we obtain $E_g = 1.819$ eV, $R = 7.7$ meV, and $\Gamma = 1.4R = 10.8$ meV. We can estimate the exciton reduced mass from our measured binding energy using the hydrogenic formula $R = 13.6m^*/\epsilon^2$ (eV) and the refractive index of 3.7 measured by Goryunova *et al.*⁸ In this way we find $m^* = 0.11m_0$, a value somewhat larger than the electron effective

mass in GaP. Since CdGeP₂ is the analog of $\frac{1}{2}(\text{InP} + \text{GaP})$ and has an energy gap midway between that of InP and GaP, it is surprising that in the effective mass in CdGeP₂ is so large and that the index is nearly as large as it is in InP. These problems are related, so that if the index of CdGeP₂ proves to be lower than 3.7, the exciton reduced mass calculated from our measurement of the binding energy would be correspondingly lower.

At photon energies above 1.83 eV, the data in Fig. 4 become progressively larger than the theoretical values describing the exciton absorption at the lowest energy gap. Sell and Lawaetz²⁵ have shown that in GaP, a similar discrepancy results from two effects: (a) the nonparabolicity of the valence bands, and (b) the onset of broadened exciton absorption at the next energy gap. Both effects should be also important in CdGeP₂, but quantitative estimates of these effects are not presently possible.

Quite apart from the determination of the exciton rydberg, the good fit between theory and experiment in Fig. 4 is significant because it is independent evidence that the dichroism of the absorption edge in II-IV-V₂ semiconductors results from the anisotropy of the A transition alone.⁷ Although transitions at the A energy gap are predominantly polarized $E \parallel Z$ by a factor of ~ 45 to 1 (see III A), the absorption for $E \perp Z$ is also dominated by the A transition, as is attested to by the appearance of an exciton at the A energy gap in Fig. 4. Estimating the amplitude of the absorption coefficient for $E \parallel Z$

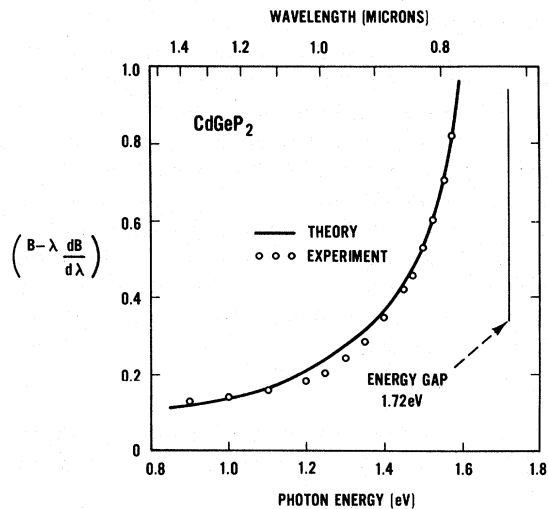


FIG. 5. Room-temperature effective birefringence of CdGeP₂ near the direct energy gap. The data are taken from Ref. 8 except for a change in sign to correct for an error in crystal orientation as discussed in the text. The theoretical curve is the expected birefringence due to the effects of the uniaxial compression on the direct energy gap.

at the energy gap by multiplying the value for $\bar{E} \perp Z$ from Fig. 4 (410 cm^{-1}) by the expected polarization ratio (45) we obtain a value of $1.85 \times 10^4 \text{ cm}^{-1}$, close to the absorption coefficient measured in III-V compounds near the energy gap at low temperatures.²²

IV. DISCUSSION

Goryunova *et al.*⁸ have recently reported measurements of the birefringence of several II-IV-V₂ compounds including CdGeP₂. These authors located the optic axis in their CdGeP₂ crystals by assuming that the intensity of light passing through a crystal was larger for $\bar{E} \parallel Z$ than for $\bar{E} \perp Z$ near the absorption edge, whereas we have seen in Fig. 3 that just the opposite is the case. Hence their conclusion that CdGeP₂ is negative birefringent is in error, and, in fact, the birefringence of CdGeP₂ is positive (extraordinary index larger than ordinary index). After allowing for this sign error, we will now show that the dispersion of the birefringence measured in CdGeP₂ can be readily explained by a theoretical model accounting for the built-in uniaxial compression alone.⁷ The amplitude of the birefringence reported by Goryunova *et al.*⁸ is also in error on account of their incorrect orientation. Since the optic axis did not lie in the plane of the crystalline slabs studied, the birefringence reported by these authors is a lower limit to the true effective birefringence of CdGeP₂.

The dispersion of the birefringence near the direct energy gap should be dominated by the polarization properties of electronic transitions at the direct energy gap. We have shown in Table I and in previous work^{1-5,7} that the splittings and polarization properties of the direct energy gap are quantitatively explained by a quasicubic model accounting for the built-in uniaxial compression alone. Hence it is reasonable to expect the dispersion of the birefringence in a chalcopyrite crystal to be the same as would obtain in its binary analog when stressed sufficiently to achieve the uniaxial distortion built into the chalcopyrite crystal. In fact, cubic crystals shatter at ten times less strain than is built into CdGeP₂, for example. We therefore represent the birefringence $B \equiv n_e - n_o$ near the energy gap as the sum of two terms:

$$B(\lambda) = B_0 + B_1(\lambda), \quad (5)$$

where $B_1(\lambda)$ is the birefringence due to the effects of the built-in compression on the fundamental band

gap and B_0 is a wavelength-independent term resulting from higher-lying band gaps and contributions to the birefringence other than the built-in compression. The quantity $B_1(\lambda)$ has been evaluated from the equations for the stress-induced birefringence of binary crystals,²⁶ using effective masses, etc., appropriate to $\frac{1}{2}(\text{GaP} + \text{InP})$, the binary analog of CdGeP₂, but using lattice constants¹⁶ appropriate to CdGeP₂. The effective birefringence $B - \lambda(dB/d\lambda)$ can then be compared with the measurements of Goryunova *et al.*⁸ The solid curve in Fig. 5 provides a good fit to the data using $B_0 = -0.005$ and arbitrarily increasing B_1 by 60%. A similar enhancement was found necessary to fit piezobirefringence data²⁶ for GaAs, and probably represents the uncertainty in our present theoretical understanding of stress-induced birefringence in binary crystals. From the good agreement in Fig. 5, we conclude that the dispersion of the birefringence near the fundamental gap results principally from the built-in compression of the chalcopyrite unit cell.

Although we have shown that this built-in uniaxial compression dominates the ordering and splittings of the valence bands as well as the dispersion of the birefringence near the direct energy gap, it does not dominate the asymptotic values of the birefringence at long wavelengths. Uniaxial compression of a large-band-gap zinc-blende crystal such as GaP produces a *negative* birefringence at long wavelengths because of a dominance of higher-lying energy gaps.²⁶ CdGeP₂ and all other II-IV-V₂ compounds^{2,27} investigated to date are *positively* birefringent. Clearly one of the other noncubic aspects of the chalcopyrite structure outlined earlier (Sec. I) is dominating the long-wavelength birefringence,²⁸ but a quantitative theory for this phenomenon is not yet available.

ACKNOWLEDGMENTS

We wish to thank G. D. Boyd, R. M. Martin, and C. K. N. Patel for several helpful discussions. We gratefully acknowledge D. D. Sell and E. O. Kane for generously providing a copy of their computer program which calculates broadened exciton absorption. We also thank Mrs. A. A. Pritchard for preparing the transverse-electroreflectance structures and L. M. Schiavone for performing the electroreflectance measurements.

¹J. L. Shay, E. Buehler, and J. H. Wernick, Phys. Rev. Letters **24**, 1301 (1970).

²J. L. Shay, E. Buehler, and J. H. Wernick, Phys. Rev. B **2**, 4104 (1970); in *Proceedings of the Tenth International Conference on the Physics of Semiconductors*, edited by S. P. Keller, J. C. Hensel, and F. Stern (U.S. Atomic Energy Commission, Oak Ridge, Tenn.,

1970), p. 589.

³J. L. Shay, E. Buehler, and J. H. Wernick, Phys. Rev. B **3**, 2004 (1971).

⁴J. L. Shay and E. Buehler, Phys. Rev. B **3**, 2598 (1971).

⁵J. E. Rowe and J. L. Shay, Phys. Rev. B **3**, 451 (1971).

⁶In Refs. 2 and 3, we discuss this mapping of the zincblende Brillouin zone into the chalcopyrite Brillouin zone and give references to the theoretical work in the Russian literature.

⁷J. L. Shay and E. Buehler, *Phys. Rev. Letters* **26**, 506 (1971).

⁸N. A. Goryunova, L. B. Zlatkin, and E. K. Ivanov, *J. Phys. Chem. Solids* **31**, 2557 (1970). These authors also ignore the distinction between birefringence ($B \equiv n_e - n_o$) and the effective birefringence [$B - \lambda(dB/d\lambda)$] determined from interference measurements. This can lead to serious errors when discussing phase matching of nonlinear interactions.

⁹N. A. Goryunova, I. I. Tychina, and R. Yu. Khansevarov, *Sov. Phys. Semicond.* **1**, 110 (1967).

¹⁰N. A. Goryunova, S. M. Ryvkin, G. P. Shpenikov, I. I. Tychina, and V. G. Fedotov, *Phys. Status Solidi* **28**, 489 (1968).

¹¹A. P. Serednii, N. A. Goryunova, I. I. Tychina, G. F. Nikolskaya, I. V. Evfimovskii, A. N. Novikova, and I. S. Kovaleva, *Phys. Status Solidi* **34**, 439 (1969).

¹²V. G. Fedotov, E. I. Leonov, V. N. Ivakhno, N. A. Goryunova, and I. I. Tychina, *Sov. Phys. Semicond.* **3**, 1470 (1970).

¹³V. Rehn and D. Kyser, *Phys. Rev. Letters* **18**, 848 (1967).

¹⁴J. J. Hopfield, *J. Phys. Chem. Solids* **15**, 97 (1960). Our sign convention for Eqs. (1) and (3) is in agreement with this reference.

¹⁵Our symmetry notation is taken from G. F. Koster, J. O. Dimmock, R. G. Wheeler, and H. Statz, *Properties of the Thirty-Two Point Groups* (MIT Press, Cambridge, Mass., 1963).

¹⁶A. S. Borshchevskii, N. A. Goryunova, F. T. Kesamanly, and D. N. Nasledov, *Phys. Status Solidi* **21**, 9 (1967).

¹⁷F. H. Pollak and M. Cardona, *Phys. Rev.* **172**, 816 (1968).

¹⁸We have taken experimental values for deformational potentials from the summary by P. Lawaetz, *Phys. Rev.* (to be published).

¹⁹N. A. Goryunova, A. S. Poplavnoi, Yu. I. Polygalov, and V. A. Chaldyshev, *Phys. Status Solidi* **39**, 9 (1970).

²⁰E. J. Johnson, in *Semiconductors and Semimetals*, edited by R. K. Willardson and A. C. Beer (Academic, New York, 1967), Vol. 3, p. 153.

²¹R. A. Forman, D. E. Aspnes, and M. Cardona, *J. Phys. Chem Solids* **31**, 227 (1970), and references cited therein.

²²M. D. Sturge, *Phys. Rev.* **127**, 768 (1962).

²³J. L. Shay, *Phys. Rev. B* **2**, 803 (1970).

²⁴T. S. Moss and T. D. F. Hawkins, *Infrared Phys.* **1**, 111 (1961).

²⁵D. D. Sell and P. Lawaetz, *Phys. Rev. Letters* **26**, 311 (1971).

²⁶C. W. Higginbotham, M. Cardona, and F. H. Pollak, *Phys. Rev.* **184**, 821 (1969); P. Y. Yu, M. Cardona, and F. H. Pollak, *Phys. Rev. B* **3**, 340 (1971).

²⁷G. D. Boyd, E. Buehler, and F. Storz, *Appl. Phys. Letters* **18**, 301 (1971).

²⁸R. M. Martin (unpublished).

Polar Mobility of Holes in III-V Compounds

J. D. Wiley

Bell Telephone Laboratories, Murray Hill, New Jersey 07974

(Received 10 May 1971)

Ehrenreich has shown that the transition probability for scattering from state \vec{k} to state \vec{k}' depends on the overlap between initial- and final-state wave functions $G(\vec{k}, \vec{k}')$. This function has been calculated for intraband and interband scattering in the p -type III-V compounds using Kane's valence-band wave functions. A simple model is proposed for polar-mode scattering in the valence bands and it is shown that the polar mobility is nearly four times larger than previously calculated for p -type III-V compounds. Approximately half of this increase is a consequence of the reduced overlap of p -like wave functions, and the other half is contributed by the presence of high-mobility carriers in the light-hole band. It is shown that the p -GaP Hall mobility data of Casey, Ermanis, and Wolfstirn can be fitted quite well throughout the lattice scattering regime and that the dominant scattering mechanisms are acoustic and nonpolar optical modes.

I. INTRODUCTION

It is well known¹⁻³ that the magnitude of the room-temperature Hall mobility in lightly doped, p -type III-V semiconductors is in good agreement with the values calculated using Ehrenreich's^{4,5} expression for polar mobility⁶ μ_{PO} . The temperature dependence of μ_{PO} is in disagreement with experiment above room temperature but this can be somewhat

improved by allowing the effective mass or dielectric constants to vary with temperature. In reporting the agreement in magnitudes, it is usually pointed out that the expression for the polar mobility contains no adjustable parameters (all the parameters being independently determined in other experiments). Thus, it is concluded, polar-mode scattering must be dominant in p -type as well as n -type III-V compounds.